

Measurement of the aperture area: an edge enhancement algorithms comparison

Pedro Bastos Costa

National Institute of Metrology, Standardization and
Industrial Quality - INMETRO
Duque de Caxias, Brazil
Universidade Federal Fluminense
Mechanical Engineering Post-Graduate Program
pbcosta@inmetro.gov.br

Fabiana Rodrigues Leta

Universidade Federal Fluminense
Mechanical Engineering Post-Graduate Program
Mechanical Engineering Department
Computational and Dimensional Metrology Laboratory
Niterói, Brazil
fabiana@ic.uff.br

Abstract — The Dimensional Metrology Laboratory of Brazilian National Institute of Metrology, Standardization and Industrial Quality (Inmetro) is developing a system for measuring the area of circular apertures used in radiometric and photometric measurements. The system is based on the visualization of the area of the aperture with a microscope and the definition of the coordinates of the edges on the captured image. Once this coordinates are obtained, the area of the aperture is calculated using an average radius. In this context it is important to choose an efficient edge enhancement algorithm. This work presents a comparison between different algorithms for edge enhancement applied in the measurement of aperture area. We also discuss the related uncertainty concerning the measurement system, evaluating these diverse algorithms.

Keywords - Edge enhancement algorithms, Aperture area, dimensional metrology, image measurement uncertainty.

I. INTRODUCTION

Recently the most changes and improvements in dimensional metrology are related to development of measurement methods with higher accuracy results and lower uncertainties.

Most of these researches are happening in development and improvement of methods and systems for non contact measurement, where all steps in the procedure are realized using computer vision techniques.

Radiometric apertures are small holes with well defined form and dimensions used to perform radiometric and photometric measurements (Fig. 1). Nowadays, these apertures area calibration is of great importance to provide accuracy and traceability for optical measurements [1, 2, 3]. The division of Optical Metrology at Inmetro is currently developing a system for the realization of the quantity of luminous intensity (candela) [4] and to achieve this purpose, the area of the radiometric apertures has to be measured with good accuracy.

Following the trend showed by the recent developments carried out by other National Metrology Institutes (NMI), the Dimensional Metrology Laboratory of Inmetro (LAMED) has also developed a non-contact measuring system for determining the area of radiometric apertures. This system differs from the traditional ones, where Coordinate

Measuring Machines (CMM) are used and the Least Squares Method applied [5].



Figure 1. Circular aperture.

It is known that pre-processing techniques can strongly alter a measurement when using digital images. For that reason we discuss in this paper the effect of using different edge enhancement algorithms in an aperture area measurement. It is highlighted the method uncertainty evaluation. This is an important analysis in any measurement process, and in general it is not considered when imaging measurement techniques are developed. The same approach can be used in other object measurement.

II. METHODOLOGY

The developed system for measuring the apertures area basically includes a microscope, an XY table, and a CCD camera. An amplified image of the aperture is captured by the camera and sent to a microcomputer. Then the x and y coordinates of the edge are determined with the aid of an algorithm, fully developed at LAMED, for enhancement of edges on images. With the coordinates of the edges it is possible to obtain an average diameter of the aperture and calculate its area.

A. Measuring software

As previously said, the developed measuring software scans the captured image in the x and y directions in order to obtain the coordinates of the points located in the edge of the aperture. These coordinates are given in numbers of pixels. The developed algorithm for this purpose is based on the analysis of the values of light intensity sensed by each pixel along an analysis line of the image. With these values, an $f(x)$ curve is modeled and the inflection points of this function indicate the pixels where the black to white transition occurs.

In other words, the inflection points permit the identification of the pixels that form the aperture edge.

B. Area computation

According to the developed mathematical model for the aperture area calculation, it is necessary to determine the coordinates of its center. These coordinates are obtained by averaging the x and y coordinates of all the points of the edge of the aperture. So it is important to highlight the aperture circumference properly, using an edge enhancement algorithm, and then becoming possible to detect the coordinates of its edge.

With the coordinates of these points and the coordinate of the center of the aperture, it is possible to define several right triangles, as shown in Fig. 2. The hypotenuses of these triangles correspond to the radius of the aperture in each measured point *i*.

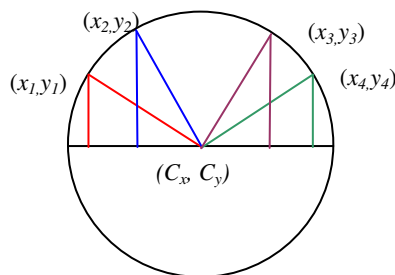


Figure 2. Schema of the aperture radius calculation.

The aperture area may be calculated using a mean radius. Thus, an expression for the area depending on the coordinates of the points of the aperture edge may be stated as shown in Eq.1.

$$A = \frac{\pi}{N} \cdot \sum_i^N [(x_i - Cx)^2 + (y_i - Cy)^2] \quad (1)$$

where (x_i, y_i) corresponds to the coordinate of a point in the aperture edge and N is the total number of points in the circle.

For the edge enhancement and the extraction of its points coordinates, the developed algorithm requires that the whole area of the aperture be within the image displayed on the screen. This requirement, associated to the algorithm and the available microscope used, restricts the utilization of the developed methodology to the measurement of apertures with diameter not greater than 10 mm.

The aim of this method is to reach better results in an aperture area calibration. Thus, six methods for edge enhancement were tested and compared each one with average value of all results. This comparison was carried out through to define if some of the methods are not appropriate for aperture area measurement. We used the following edge enhancement algorithms: Sobel, Prewitt, Roberts, Laplacian, Zero-Crossing and Canny [6] [7].

The obtained results of these six methods are showed in Fig. 3. It is possible to note that the not all the filters sharpen completely the aperture border. In those cases it is necessary to interpolate new points along the edge, allowing the perimeter detection.

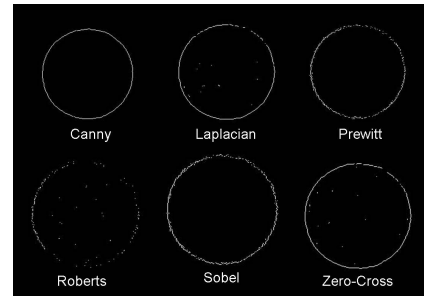


Figure 3. Edge enhancement algorithms results.

III – MEASUREMENT AND RESULTS

To analyze the algorithm performance for circular aperture measurements, two diameter apertures (8 mm and 3 mm) were measured, in accordance with the method described in II. The Table 1 and Fig. 4 show the area results for an aperture of 8 mm and their respective uncertainties (see section IV).

TABLE 1. OBTAINED AREA AND UNCERTAINTY: 8MM DIAMETER

Method	Area(mm ²)	Uncertainty (mm ²)
Sobel	49,642	0,859
Prewitt	49,824	0,856
Roberts	50,346	0,865
Laplacian	50,012	0,845
Zero-Crossing	49,949	0,843
Canny	50,122	0,844

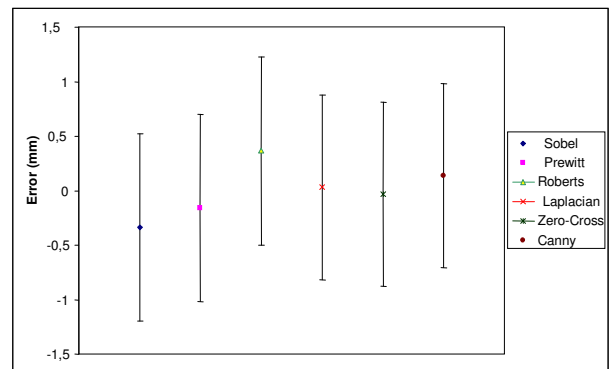


Figure 4. Results of 8 mm aperture.

The second test was carried out in an aperture with a 3 mm diameter. The objective was to obtain lower uncertainty and to compare values with small differences. The results are shown in Table 2 and Fig. 5.

TABLE 2. OBTAINED AREA AND UNCERTAINTY: 3MM DIAMETER

Method	Area(mm ²)	Uncertainty (mm ²)
Sobel	7,281	0,313
Prewitt	7,366	0,304
Roberts	7,313	0,304
Laplacian	7,230	0,304
Zero-Crossing	7,237	0,304
Canny	7,263	0,304

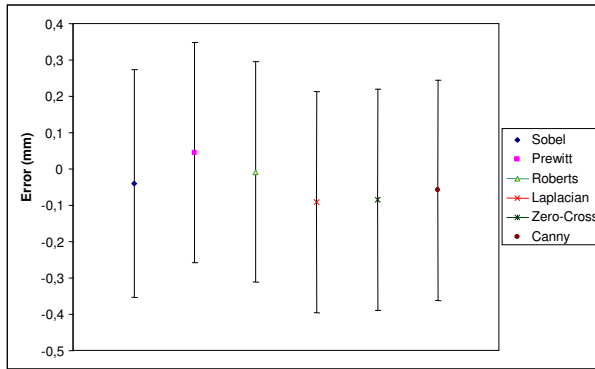


Figure 5. Results of 3 mm aperture.

IV. UNCERTAINTY EVALUATION

The mathematical model used to obtain the final value of the area and evaluate the measurement uncertainty derives from Eq. 1. However, the results of this equation as presented are given in pixels. In order to obtain values in area unit, it is necessary to define the length of the pixel, that is, to determine how much a pixel of the displayed image represents in units of length. This length was defined with aid of a laser interferometer. The final mathematical model to obtain the aperture area in length units is shown in Eq. 2. In this expression, the thermal expansion effect of the component during the measurement is also considered.

$$A_{(Aperture)} = \frac{\pi \cdot \{ [(x_i - C_x) \cdot L_{px}]^2 + [(y_i - C_y) \cdot L_{py}]^2 \}}{1 + \beta \cdot \Delta t} \quad (2)$$

Where the presented variables are defined as below:

- x_i Edge coordinates in x direction (in pixels)
- C_x Circumference center coordinate in x-axis (in pixels)
- L_{px} Pixel length in x direction
- y_i Edge coordinates in y direction (in pixels)
- C_y Circumference center coordinate in y-axis (in pixels)
- L_{py} Pixel length in y direction
- β Surface thermal expansion coefficient
- Δt Aperture temperature deviation from the 20°C, which is the reference temperature

A. Type A standard uncertainty

According to the proposed measurement procedure, the aperture was scanned in five different positions and 3000 points of its edge were measured. With the coordinates of the center of the aperture and the coordinates of each measured point a correspondent value of the aperture area is calculated. The measurement repeatability was estimated by the standard deviation of these calculated values of area. This component of uncertainty, though, is small when compared to the other contributions since the number of measured points is very large.

As an example, the values for the measurement of a 3 mm diameter aperture are presented. An average aperture area of 7,281 mm² was obtained. The standard deviation of the repeated measurements was of 0.081mm². The repeatability was determined according to Eq. 3, as stated in [6].

$$u(A) = \frac{s}{\sqrt{n}} \quad (3)$$

Thus, the measurements results repeatability is 0,001 mm².

B. Type B standard uncertainties

From the analysis of the mathematical model, it can be found that the main sources of type B uncertainty are related to: the accurate definition of the pixels that are located on the edge of the aperture; the calculation of the center of the aperture; the determination of the length of the pixels; the temperature variations and the variations of the thermal expansion coefficient. To evaluate the combined standard uncertainty, an estimative for each of these sources of uncertainty was established. The calculus procedure showed below is just for uncertainties related to the image processing.

C. Edge x coordinate uncertainty

The uncertainties associated to the coordinates of the aperture edge in the x-axis are estimated as the maximum possible error of the developed algorithm when recognizing a point on the aperture edge.

This error, on its turn, is considered to be half of a pixel, because if the aperture edge is not exactly located in the intersection of two pixels but in the middle of a pixel, the algorithm will automatically detect the aperture edge as being located in one of the extremities of this pixel. A rectangular distribution is attributed to this error since the probability of the aperture edge to be located in a certain point inside a given pixel is the same for all the points of this pixel. The sensitivity coefficient is calculated by means of Eq. 4.

$$\frac{\partial A}{\partial x_i} = 2\pi \cdot (x_i - C_x) \cdot \frac{L_{px}^2}{1 + \beta \cdot \Delta t} \quad (4)$$

D. Edge y coordinate uncertainty

The uncertainty in the determination of the y coordinates of the edge points is analogous to the uncertainty evaluation of the x coordinates. Thus, the same considerations presented in previous section may be applied here. The analogous sensitivity coefficient is shown in Eq. 5.

$$\frac{\partial A}{\partial y_i} = 2\pi \cdot (y_i - C_y) \cdot \frac{L_{py}^2}{1 + \beta \cdot \Delta t} \quad (5)$$

E. Pixel length uncertainty

The pixel lengths relative to the axes x and y are obtained with a previous calibration of the image. In the system applied at LAMED, the calibrated pixels have dimensions of 0,017 mm for both axes x and y. These conventional values have associated expanded uncertainties of 20 nm, calculated with a coverage factor $k = 2$.

The sensitivity coefficients that represent the variation of the calculated area in relation to the pixel lengths are obtained according to Eq. 6 and Eq. 7.

$$\frac{\partial A}{\partial L_{px}} = 2\pi \cdot (x_i - C_x)^2 \cdot \frac{L_{px}}{1 + \beta \cdot \Delta t} \quad (6)$$

$$\frac{\partial A}{\partial L_{py}} = 2\pi \cdot (y_i - C_y)^2 \cdot \frac{L_{py}}{1 + \beta \cdot \Delta t} \quad (7)$$

In the presented equations, it can be seen that the $\partial A/\partial L_p$ coefficients are dependent on the square of the differences between the coordinates of the points located on the edge and the points of the center of the aperture. As the value of these differences is very significant when compared to the remaining quantities, it is expected that the component of uncertainty associated to the determination of the pixel length (L_p) will exert one of the biggest contributions for the combined uncertainty. Moreover, the bigger is the diameter of the aperture, the bigger will be the contribution of this component of uncertainty, and, consequently, the bigger will be the combined uncertainty.

F. Combined standard uncertainty

The combined standard uncertainty associated to the area of diameter aperture was calculated according to Eq. 8. The values of the terms of this equation are presented in Table 3.

$$u_c^2(A) = \left[\frac{\partial A}{\partial x_i} \right]^2 \cdot u^2(x_i) + \left[\frac{\partial A}{\partial y_i} \right]^2 \cdot u^2(y_i) + \left[\frac{\partial A}{\partial C_x} \right]^2 \cdot u^2(C_x) + \left[\frac{\partial A}{\partial C_y} \right]^2 \cdot u^2(C_y) + \left[\frac{\partial A}{\partial L_{px}} \right]^2 \cdot u^2(L_{px}) + \left[\frac{\partial A}{\partial L_{py}} \right]^2 \cdot u^2(L_{py}) + \left[\frac{\partial A}{\partial \beta} \right]^2 \cdot u^2(\beta) + \left[\frac{\partial A}{\partial \Delta t} \right]^2 \cdot u^2(\Delta t) + 2 \cdot \left[\left(\frac{\partial A}{\partial x_i} \cdot \frac{\partial A}{\partial C_x} \cdot u(x_i) \cdot u(C_x) \cdot r(x_i, C_x) \right) + \left(\frac{\partial A}{\partial y_i} \cdot \frac{\partial A}{\partial C_y} \cdot u(y_i) \cdot u(C_y) \cdot r(y_i, C_y) \right) \right] \quad (8)$$

Equation 8 expresses the *uncertainty propagation law*, as stated in [8], and includes all the input quantities from which the area is derived and the influence quantities that significantly affect the final result. The last two terms of this equation take into account the correlation between two input quantities.

TABLE 3. UNCERTAINTY EVALUATION

Standard Uncertainty Component	Probability distribution	Standard uncertainty value - U(x _i)	Degrees of freedom - ν _i	Sensitivity coefficients - c _i	uA(x _i) ≡ c _i ·u(x _i) mm ²
u(x)	R	0,289	Infinite	7E-4 mm ²	0,004
u(y)	R	0,289	Infinite	7E-4 mm ²	0,004
u(C _x)	N	2,5	169	-6.9E-4 mm ²	0,001
u(C _y)	N	2,25	169	-7.1E-4 mm ²	0,001
u(Ā)	N	30 (nm ²)	3849	1	0,00003
u(Δt)	R	0.006 (°C)	Infinite	2.1E-6 mm ² / °C	1,21E-08
	R	0.069 (°C)	Infinite	2.19E-6 mm ² / °C	1,45E-07
u(β)	R	1E-05 (1/°C)	50	-1.1E-2 mm ² · °C	6,30E-08
u(L _{px})	N	10 (nm)	Infinite	98 mm	0,006
u(L _{py})	N	10 (nm)	Infinite	99 mm	0,006

Note: R – rectangular probability distribution, N – normal probability distribution

The correlation was calculated according to Eq. 9 and Eq. 10. An estimative of the variation in the center coordinates (δ_{C_x} and δ_{C_y}) was obtained by generating a variation in the inputs, that is, in the edges coordinates (δ_{x_i} and δ_{y_i}) and observing the resulting effect on the determination of the center.

$$r(x_i, C_x) \approx \frac{u(x_i) \cdot \delta_{C_x}}{u(C_x) \cdot \delta_{x_i}} = 1,33E - 09 \quad (9)$$

$$r(x_i, C_y) \approx \frac{u(y_i) \cdot \delta_{C_y}}{u(C_y) \cdot \delta_{y_i}} = 1,38E - 09 \quad (10)$$

G. Expanded uncertainty

The expanded uncertainty was obtained using a coverage factor of 2 ($k = 2$) with 95,45% confidence level. This factor derives from the calculation of the effective freedom degrees of $u_c(A)$, such as presented in Eq. 11. Also, it is assumed that the output quantity is characterized by a normal distribution. Thus, the

coverage factor was selected according to the parameters of the *t*-distribution.

$$\nu_{eff} = \frac{u_c^4}{\frac{u^4(A)}{3000} + \frac{u^4(C_x)}{169} + \frac{u^4(C_y)}{169} + \frac{u^4(\beta)}{50}} = 623,7 \quad (11)$$

V – CONCLUSION

With the proposed method, the Dimensional Metrology Laboratory of Inmetro is able to attend the demands for the calibration of aperture areas with an adequate accuracy since the expanded uncertainty for the measured apertures is compatible with the accuracy required by the photometric and radiometric measurements performed at this institute. Thus, this calibration procedure provides national traceability for these standards, and consequently, for the radiometric and photometric measurements.

The results obtained with all algorithms were considered very satisfactory, once the differences between all values were lower than the uncertainty of measurement in both cases.

The algorithm chosen to be used as reference for the circular aperture measurements was the Canny method. With this algorithm the images presented better definition of the edges, diminishing the number of incorrect values in the enhancement of the aperture edges.

ACKNOWLEDGMENT

The second author thanks FAPERJ for the financial support (No. E-26/171.362/2001).

REFERENCES

- [1] E. Ikonen, P. Toivanen and A. Lassila, "A new optical method for high-accuracy determination of aperture area", *Metrologia*, vol. 35, pp. 369-372, 1998.
- [2] J. Fowler and M. Litorja, "Geometric area measurement of circular apertures for radiometry at NIST", *Metrologia*, vol. 40, pp. S9-S12, 2003.
- [3] J. A. Fedchak, A. C. Carter, R. Datla. Measurement of small apertures. *Metrologia*, 43, pp. S41-S45, 2006.
- [4] L. Alves, C. Coelho, F. Reis, P. Costa, "Análise da medição da área de abertura para a realização da candela", *1º Congresso internacional de metrologia mecânica*, Rio de Janeiro, Brazil, Oct. 2008.
- [5] A. Rezet, "Analytical resolution of Least-Square applications for the circle in interferometry and radiometry", *Metrologia*, vol. 35, pp. 143-149, 1998.
- [6] A. Conci, E. Azevedo and F. R. Leta, *Computação Gráfica – Teoria e Prática*, [v.2]. Rio de Janeiro. Brazil. Elsevier Editora Ltda, 2008.
- [7] A. Bovik (ed.), *Handbook of Image & Video*, 2nd ed. USA. Elsevier Academic Press, 2005.
- [8] ISO - International Organization for Standardization, *Guide to the expression of uncertainty in measurement*. First edition, corrected and reprinted, Switzerland, 1995.